**Astronomy
&
Astrophysics**

Kinetic equilibrium of iron in the atmospheres of cool stars

III. The ionization equilibrium of selected reference stars⋆

A. J. Korn[1,2], J. Shi[1,3], and T. Gehren[1]

[1] Institut für Astronomie und Astrophysik der Universität München, Universitäts-Sternwarte München (USM),
Scheinerstraße 1, 81679 München, Germany
[2] Max-Planck Institut für extraterrestrische Physik (MPE), Giessenbachstraße, 85748 Garching, Germany
[3] National Astronomical Observatories, Chinese Academy of Sciences (NAOC), Beijing 100012, PR China

Abstract. Non-LTE line formation calculations of Fe I are performed for a small number of reference stars to investigate and quantify the efficiency of neutral hydrogen collisions. Using the atomic model that was described in previous publications, the final discrimination with respect to hydrogen collisions is based on the condition that the surface gravities as determined by the Fe I/Fe II ionization equilibria are in agreement with their astrometric counterparts obtained from HIPPARCOS parallaxes.
High signal-to-noise, high-resolution échelle spectra are analysed to determine individual profile fits and differential abundances of iron lines. Depending on the choice of the hydrogen collision scaling factor S_H, we find deviations from LTE in Fe I ranging from 0.00 ($S_H = \infty$) to 0.46 dex ($S_H = 0$ for HD 140283) in the logarithmic abundances while Fe II follows LTE. With the exception of Procyon, for which a mild temperature correction is needed to fulfil the ionization balance, excellent consistency is obtained for the metal-poor reference stars if Balmer profile temperatures are combined with $S_H = 3$. This value is much higher than what is found for simple atoms like Li or Ca, both from laboratory measurements and inference of stellar analyses. The correct choice of collisional damping parameters ("van-der-Waals" constants) is found to be generally more important for these little evolved metal-poor stars than considering departures from LTE. For the Sun the calibrated value for S_H leads to average Fe I non-LTE corrections of 0.02 dex and a mean abundance from Fe I lines of $\log \varepsilon(\text{Fe}) = 7.49 \pm 0.08$.
We confront the deduced stellar parameters with comparable spectroscopic analyses by other authors which also rely on the iron ionization equilibrium as a gravity indicator. On the basis of the HIPPARCOS astrometry our results are shown to be an order of magnitude more precise than published data sets, both in terms of offset and star-to-star scatter.

Key words. line: formation – Sun: abundances – stars: fundamental parameters – stars: abundances – stars: individual: HD 140283 – stars: individual: Procyon

1. Introduction

As is evident from our previous investigations (Gehren et al. 2001a, b), the large scatter among laboratory f values of neutral iron lines does not allow the unambiguous determination of a kinetic model of the iron atom in the solar atmosphere. In particular, the rôle of collisions with neutral hydrogen atoms could not be fully explored. This resulted in an uncertainty of the hydrogen collision scaling factor S_H (a multiplicative modification to the Drawin 1968, 1969 formula for allowed inelastic collisions with neutral hydrogen) which becomes important as soon as the kinetic model is applied to metal-poor stars. Since in the atmospheres of halo and thick disk stars

line-blanketing in the UV becomes more and more unimportant leading to an increase of photoionization, while simultaneously electron collisions can no longer counterbalance the predominance of radiation interactions, the hydrogen collisions are an essential part of the kinetic equilibrium of iron, and many other photoionization-dominated metals as well. This problem is further enhanced by the new radiative cross-sections of Bautista (1997) which are substantially larger than simple hydrogenic approximations would make believe.

To establish the influence of deviations from LTE on the *ionization equilibrium* of iron we have therefore chosen a number of *reference stars* which we feel are sufficiently representative of the local metal-poor stellar generation on and near the main sequence. Our interest is particularly devoted to the important question: to what extent is the derivation of spectroscopic stellar parameters and metallicities affected by the kinetic equilibrium of iron? Answering this question involves the

Table 1. Basic stellar parameters of the reference stars. The iron abundance is derived from Fe II lines with the microturbulence fulfilling the usual line strength constraint (see text). $[\alpha/\text{Fe}] = 0.4$ was adopted in the computation of the metal-poor atmospheres, for Procyon ($\equiv$ HD 61421) a solar mixture was assumed. Except for Procyon (data from Allende Prieto et al. 2002), surface gravities are from HIPPARCOS parallaxes with masses derived from the tracks of VandenBerg et al. (2000). $[\text{Fe/H}] = \log(\text{Fe/H})_\star - \log(\text{Fe/H})_\odot$.

Star	T_{eff} [K]	$\log g$ (cgs)	[Fe/H]	ξ [km s^{-1}]	π_{HIP} ['']	M [$M_\odot$]
HD 103095	5070	4.69	−1.35	0.95	109.2	0.62
HD 19445	6032	4.40	−2.08	1.75	25.9	0.67
HD 140283[1]	5806	3.69	−2.42	1.70	17.4	0.79
HD 84937[1]	6346	4.00	−2.16	1.80	12.4	0.79
Procyon	6510	3.96	−0.03	1.83	285.9	1.42
Sun	5780	4.44	0.0	1.0	–	1.00

[1] For this star extinction due to interstellar reddening was considered following Hauck & Mermilliod (1998, cf. Table 7).

investigation of the radiation field (depending mostly on the effective temperature) and of the collisional interaction (depending mostly on surface gravity). Therefore our choice of metal-poor reference stars has led to four representatives: HD 103095 ($\equiv$ Gmb 1830) as a cool main sequence star, HD 19445 as a typical subdwarf, HD 84937 as a turnoff star and HD 140283 as a moderately cool subgiant. The last two of these reference stars have also been chosen by Asplund et al. (2000) to model hydrodynamic convection in metal-poor stars.

Photospheric surface gravities are usually determined by means of three independent methods. In principle the most reliable approach uses astrometry (presently the HIPPARCOS parallaxes, ESA 1997) with an appropriate guess of the stellar mass, which enters the resulting $\log g$ only with a $\sigma(\log M)$ uncertainty. Since the mass uncertainty of these very old stars is generally below $0.05\,M_\odot$ (when referring to a given set of evolutionary tracks), the corresponding error stays below 0.03. The uncertainty of the effective temperature enters as $4\,\sigma(\log T_{\text{eff}}) \approx 0.02$. Thus the prime error in $\log g$ is due to that of the parallax itself ($2\,\sigma(\log \pi)$), which for the four stars is between 0.01 (Gmb 1830) and 0.07 (HD 84937). The maximum error then is between 0.06 and 0.12 in $\log g$.

The second method refers to the *damping wings* of strong neutral metal lines such as the Mg Ib triplet. However, as demonstrated by Fuhrmann (1998a), for stars with $[\text{Fe/H}] < -2$ the wings of such lines become extremely shallow and the determination correspondingly uncertain. The combination of Balmer profile temperatures and Mg Ib gravities (both in LTE) was shown to be fully compatible with the HIPPARCOS astrometry (Fuhrmann 1998b, 2003).

Originally, the surface gravity of remote subdwarfs and subgiants was derived from the *ionization equilibrium* of iron where for simplicity and lack of better evidence one used the assumption that Fe I/Fe II is populated according to the Saha/Boltzmann equilibrium (LTE). For a number of stars including Procyon as a primary standard this was shown to lead

to results incompatible with those obtained from strong line wings (Fuhrmann et al. 1997) or HIPPARCOS parallaxes. More specifically, evolutionary stages are predicted which have not yet been reached. Therefore, the present approach has abandoned the LTE assumption and obtains the surface gravity from a fit to the Fe lines in kinetic equilibrium.

To evaluate the reliability of the non-LTE calculations in stars with different parameters Procyon ($\equiv \alpha$ CMi) was also selected, because the discrepancy between $\log g$ obtained from ionization equilibrium and parallax remains unresolved.

Table 1 lists the basic stellar parameters of the five stars plus the Sun.

2. Observations

Spectra of the stars were taken with the fibre-fed échelle spectrograph FOCES (Pfeiffer et al. 1998) at the 2.2-m telescope of the German-Spanish Astronomical Centre on Calar Alto during a number of observing runs between 1999 and 2001, with a spectral resolution of $R = 65\,000$ (HD 140283 was observed at $R = 40\,000$). As measured in line-free spectral windows near Hα, the peak signal-to-noise ratio (S/N) exceeds 300:1 in all cases. With a spectral coverage of 4200–9000 Å our analyses naturally focus on the lines of Fe I and Fe II in the visible disregarding the resonance lines in the (near) UV.

Owing to the design of FOCES (the light of both star and flatfield lamp being transmitted through the same optical path), the resulting flatfield calibration of the stellar spectra produces an extremely predictable continuum run that contains only the remaining second-order variation with wavelength which results from the difference between stellar T_{eff} and the temperature of the halogen lamp. The internal accuracy of the effective temperature determination is therefore very high, with profile residuals well below 0.5% of the continuum (cf. Korn 2002). The profile analysis of metal lines also profits from this quality, especially when the line density is high.

3. Stellar effective temperatures and gravities

The temperature scale adopted is based on Balmer line-broadening theory combined from Stark effect profiles of Vidal et al. (1970) and the Ali & Griem (1965, 1966) approximation of resonance broadening (see Fuhrmann et al. 1993). The basis of this approach was the different relative contributions of these broadening processes to Hα on the one hand (essentially broadened by H collisions) and the higher series members (dominated by the Stark effect) on the other. The results have been fixed with a minimum number of free parameters for solar-type stars with ranging metallicities based on empirical evidence. Weights are assigned to the temperatures derived from each line based on temperature sensitivity, S/N and blaze correction reliability. At present we refrain from adopting the recent hydrogen line-broadening theory of Barklem et al. (2000). As our own implementation shows, it does not reproduce the solar temperature to within 100 K (using the MARCS code and a χ^2 fitting technique which allows for the intersection of observed profiles this value is 50 K, Barklem et al. 2000). In addition, it fails to reproduce the profile shape of higher Balmer lines

Table 2. Comparison of effective temperature determinations for the five reference stars. TI99 = Thévenin & Idiart (1999), F00 = Fulbright (2000), AAM-R96 = Alonso et al. (1996), GCC96 = Gratton et al. (1996), KSG03 = this work. The mean offset is computed for the four metal-poor stars according to ΔT_{eff} (study – KSG03). Significant offsets with respect to our temperature scale are encountered in the studies of Thévenin & Idiart (1999) and Fulbright (2000).

Star	TI99 $B-V$	F00 EE[1]	AAM-R96 IRFM	GCC96 IRFM	KSG03 Balmer
HD 103095	4990	4950	5029	5124	5070
HD 19445	5860	5825	6050	6066[2]	6032
HD 140283	5600	5650	5691	5766[3]	5806
HD 84937	6222	6375	6330	6351[2]	6346
Mean offset	−146	−114	−39	+13	±0
Procyon	6631	–	6579	–	6508

[1] EE = excitation equilibrium of Fe I in LTE.
[2] Average T_{eff} of two analyses.
[3] Average T_{eff} of three analyses.

(Hβ and up) of stars like HD 140283 and HD 19445, both of which are located in the temperature band where differences between the two broadening theories are expected to be largest.

We utilize the atmospheric model MAFAGS (Fuhrmann et al. 1997) which is line-blanketed by means of the Kurucz ODFs (Kurucz 1992). Note that these ODFs were computed assuming[1] $\log \varepsilon(\text{Fe}) = 7.67$. We therefore rescale them by -0.16 dex to account for the low Solar iron abundance of $\log \varepsilon(\text{Fe}) = 7.51$. Unlike in other widely-used atmospheric codes like ATLAS or MARCS, we use a mixing length $\alpha = l/H_{\text{p}} = 0.5$ in the framework of the Böhm-Vitense (1958) theory of convection in order to bring Hα and the higher Balmer lines into concordance. The differences with respect to other methods of temperature determination have been described in Fuhrmann et al. (1993) and Fuhrmann (1998b). We note that the choice of the mixing-length affects the Balmer lines, but the influence on the Fe I and Fe II lines analysed in the Sun turns out to be equivalent to $\Delta \log \varepsilon_{\text{Fe}} < 0.01$ dex. The same is true for metal-poor stellar atmospheres such as that of HD 140283. It also holds for the corresponding non-LTE computations.

The temperature scale resulting from our hydrogen line profile fitting is *higher* for the metal-poor stars than the photometric one of Thévenin & Idiart (1999) and Fulbright (2000) by more than 100 K. It is, however, in excellent agreement with the infrared flux method (IRFM) temperatures of Alonso et al. (1996) and Gratton et al. (1996). Table 2 confronts the corresponding numbers in detail. Only HD 140283 displays a markedly lower temperature in the Alonso et al. calibration. This is, at least in part, due to the zero-reddening assumption adopted by these authors. A discussion of this point can be found in Fuhrmann (1998a).

Yet another independent temperature scale seems to support the Balmer profile temperatures: Peterson et al. (2001) derive temperatures for HD 19445 and HD 84937 (and other

___
[1] $\log \varepsilon(\text{Fe}) = \log (n_{\text{Fe}}/n_{\text{H}}) + 12$.

stars) from absolute fluxes in the mid-UV. Effective temperatures of 6050 K and 6300 K were obtained. Peterson (2003, priv. comm.) analysed HD 140283 with similar methods obtaining 5850 K. In total the mean offset between our temperature scales is thus well below 10 K.

For the calibration the surface gravity is taken from HIPPARCOS parallaxes. Additional quantities entering the equation are taken from Alonso et al. (1996, bolometric correction BC), Hauck & Mermilliod (1998, interstellar extinction A_V) and VandenBerg et al. (2000, stellar mass M). To derive the latter, the star is placed among the evolutionary tracks appropriately chosen with respect to metallicity ([Fe/H]$_{\text{NLTE}}$) and α-enhancement ([O/Fe]$_{\text{NLTE}}$, according to Reetz 1999). This process is iterated to convergence.

After the calibration the final atomic model (which best reproduces the astrometric results *on average*) is used to derive gravities which can then be compared with HIPPARCOS to quantify the star-to-star scatter.

4. Metal-poor reference stars and Procyon

As described in Papers I and II in considerable detail, our present approach to the analysis of the reference stars is based on a number of assumptions.

Atmospheric models are calculated for all stars (including the Sun) according to the same type of input parameters, boundary conditions, and constraint equations. We thus intentionally avoid the use of empirical models.

The major orientation of our analysis is that of *empirical* evidence. Although some theoretical model descriptions appear more satisfactory than others, we build upon the experience that shortcomings in theories can be detected only by comparison with observations.

Our basic approach to stellar spectroscopy is differential in the sense that we require all types of input physics to be in agreement with solar observations. This requirement clearly dictates the individual line fit approach, and it excludes the use of absolute f values. It is important to recognize that the typical abundance scatter obtained from solar spectral analysis of Fe lines is considerably higher than warranted by both observational error and differences in theoretical models. There are essentially two explanations for this result: either the f values are not reliable or a significant fraction of Fe lines are contaminated by relatively strong (yet undetected) blends.

Differential spectrum analysis must account for line broadening, particularly when solar-type and extremely metal-poor stars are to be compared. This is in fact the most important constraint because it involves additional atomic parameters and line broadening theories. Every strategy to deal with strong line wings automatically involves the problems of atmospheric modelling. Consequently, for interpretation we establish steps of decreasing reliability with constraints coming from the observed line profile and the concept that the solar photospheric abundance of Fe is the same for all lines. Purely radiative parameters (f values) are complemented by collisional broadening (Stark effect, van der Waals-type damping). The variety of line strengths observed in the solar spectrum then provides a comparison between weak and strong lines of

the resulting abundances, with all f values taken from laboratory measurements and the damping constants adjusted for the strong lines to minimize trends with line strength (see Paper II). Although this interferes occasionally with thermal or microturbulent broadening velocities, Doppler broadening can be generally separated from the influence of damping wings. As a result, stellar line abundances are compared with the individual abundances of their solar counterparts. This is what is often called a line-by-line differential (non-)LTE analysis.

The line broadening problems are less significant for a differential analysis of Fe II lines, however, here Doppler broadening plays an important role. The scatter introduced to the solar Fe II abundance by the various data sets is even higher than for Fe I thus a differential approach is absolutely necessary.

The above considerations of the different contributions to line formation severely limit the possible conclusions. Still, experience with stellar analyses show that atomic data are in many cases better determined from the solar spectrum than from a terrestrial laboratory.

4.1. Non-LTE calculations

With little progress in the understanding of the physics of hydrogen collisions, the review of Lambert (1993) still reflects our current state of knowledge. While the energy range encountered in stellar atmospheres is not accessible to experiment, Lambert concludes from measurements at 15 eV that the Drawin (1968, 1969) formula most likely overestimates the true efficiency of this thermalizing process by two orders of magnitude. If this was the case, they could safely be disregarded. Rather than assuming that hydrogen collisions are inefficient all together, we take on the view of Steenbock & Holweger (1984) that the "*lack of reliable collision cross-sections constitutes a major problem in statistical-equilibrium studies of cool stars*". To face this problem we keep the efficiency of hydrogen collisions S_H as a free parameter which must be determined by appropriate observations.

As would be predicted, electron collisions cannot contribute very much to thermalization, since the density of free electrons is roughly a factor 10 smaller than in comparable stars of solar metal content. Our calculations support this idea fully. In metal-poor stars therefore no other process but hydrogen collisions can – at least to some extent and depending on their cross-section – compensate for the high photoionization rates which would otherwise lead to extreme overionization at variance with the spectroscopic evidence given below. It is of course unsatisfactory to use such a rather primitive representation of the collision process as the Drawin approximation which was never meant to be extended to anything else but collisions between rare gases. There is, however, a similar behaviour of both formulae of van Regemorter (1962, for electron collisions) and Drawin (for hydrogen collisions) in that the rates for both types of thermalization are proportional to the f value and both depend on the inverse threshold energy. Such a variation leads to a general increase of collision rates with excitation energy, because highly excited levels cluster near the ionization limit. Solar photospheric emission lines

show at least for Mg I and Al I that it is just these highly excited levels which lead to Rydberg transitions dominated by a population inversion. This requires low collision rates (whether electron or hydrogen) for such transitions, and in fact the corresponding hydrogen collision factors for such atomic models were found to fit the observed emission lines with S_H values significantly below unity (Baumüller & Gehren 1996; Zhao et al. 1998). Carlsson et al. (1992) reproduce the IR emission lines entirely without hydrogen collisions, but do not simultaneously model the optical absorption lines.

For Fe, we determine S_H by requiring that both Fe I and Fe II lines produce a single-valued mean iron abundance when the gravity is assumed to be that derived from the HIPPARCOS parallax. This leaves the hydrogen collision enhancement factor S_H as the single free parameter in this investigation.

A number of non-LTE test calculations with various choices for S_H was performed for the reference stars, together with LTE calculations. Line profiles were fitted using external Gaussian broadening profiles essentially defined by the instrumental resolution. While the intrinsic profiles are better reproduced by a radial-tangential approximation to macroturbulence (Gray 1977), the dominance of the instrumental resolution and the relative weakness of the iron lines considered ($W_\lambda < 100$ mÅ) justify the use of a Gaussian. Equivalent widths (EWs) are then computed from the theoretical spectra to constrain the microturbulence ξ. Thus EWs only enter the analysis for the derivation of ξ, all other aspects are performed using line profiles. The corresponding data is presented in Tables 4 and 5.

4.2. Evidence for non-vanishing hydrogen collisions: The subgiant HD 140283

The dynamic range of Fe I abundances in HD 140283 upon varying S_H is exemplified by Fig. 1 and Table 3: the extreme underpopulation of Fe I in its atmosphere is clearly seen. The depopulation with respect to the LTE case already starts in deep photospheric layers. For vanishing S_H the departure coefficients b_i drop to 0.5 near $\log \tau = -0.5$.

Models with $S_H > 0$ produce less extreme departures as radiative processes (photoionization) are increasingly compensated for by collisional ones (hydrogen collisions). More importantly, though, a non-vanishing S_H secures *relative thermal excitation equilibrium*: although strongly overionized with respect to Fe II, the Fe I populations are kept thermal relative to one another, even by collisional efficiencies lower than indicated by the Drawin formula (e.g. $S_H = 0.1$). Since only the ratio of the departure coefficients enters the line source function S_ν^l, identical b_i result in a Planckian S_ν^l. This means that within a given model non-LTE corrections only depend on the contribution function, i.e. the depth of formation. Thus low-excitation lines will experience larger corrections on average.

Calculations including hydrogen collisions then constitute a model sequence with non-LTE abundance corrections steadily decreasing with an increasing value for S_H. The behaviour found in the metal-poor stars is morphologically

Table 3. Fe I and Fe II abundances for the reference stars and the Sun for different assumptions concerning the efficiency of hydrogen collisions. Differential abundances [Fe/H]$_{diff}$ are given, except in the case of the Sun where $\log \varepsilon$(Fe) is specified. σ refers to the line-to-line scatter which is a factor $\sqrt{n}$ larger than the error of the mean. Note that the scatter in [Fe II/H]$_{diff}$ is significantly reduced. Like in the case of HD 140283 discussed above, a strong imbalance between Fe I and Fe II results for all metal-poor stars if $S_H = 0$ is assumed. Instead, the ionization equilibrium points towards $S_H = 3$. Procyon cannot be fitted by any model.

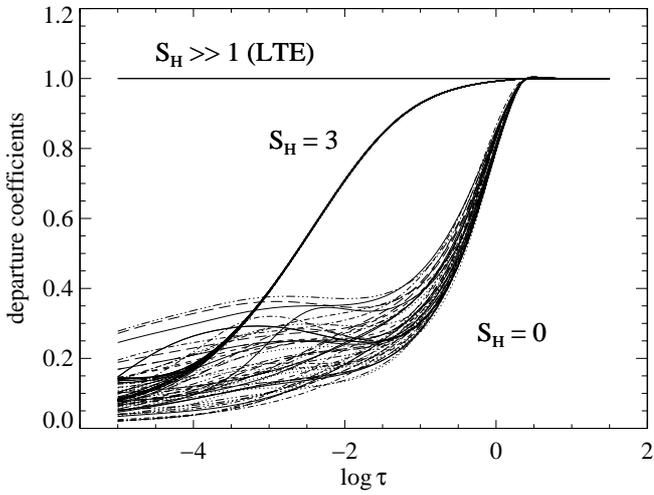| Object	$S_H = 0$ [Fe I/H] $\pm \sigma$	$S_H = 3$ [Fe I/H] $\pm \sigma$	LTE [Fe I/H] $\pm \sigma$	# of lines	LTE [Fe II/H] $\pm \sigma$	# of lines
HD 103095	-1.21 ± 0.03	-1.35 ± 0.04	-1.33 ± 0.04	41	-1.36 ± 0.03	15
HD19445	-1.67 ± 0.07	-2.07 ± 0.08	-2.07 ± 0.08	58	-2.08 ± 0.05	16
HD 140283	-2.00 ± 0.07	-2.43 ± 0.09	-2.46 ± 0.09	62	-2.43 ± 0.05	13
HD 84937	-1.78 ± 0.07	-2.15 ± 0.09	-2.18 ± 0.09	61	-2.16 ± 0.05	16
Procyon	-0.08 ± 0.06	-0.10 ± 0.08	-0.11 ± 0.07	52	-0.03 ± 0.04	23
Sun	7.54 ± 0.08	7.49 ± 0.08	7.46 ± 0.07	96	7.53 ± 0.10	37

Fig. 1. Departure coefficients b_i for Fe I terms in HD 140283 as a function of the optical depth $\log \tau_{5000}$. It becomes evident that they depend drastically on S_H. The line source functions are Planckian for all models with $S_H > 0$, but not for the $S_H = 0$ model. The best model ($S_H = 3$) already returns abundances quite close to LTE.

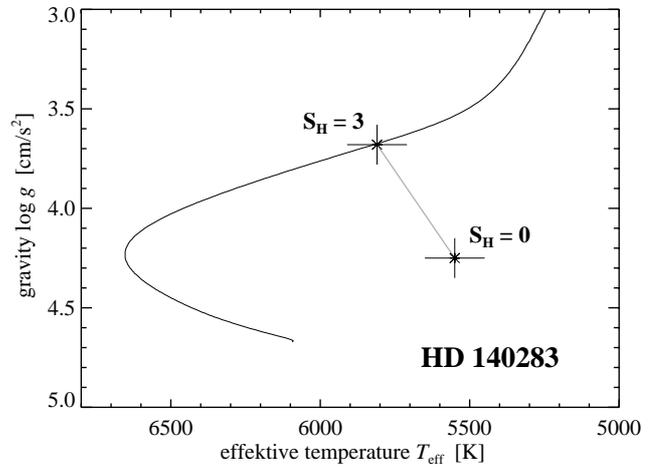**Fig. 2.** A comparison between the stellar parameters of HD 140283 for different assumptions concerning the efficiency of hydrogen collisions. $S_H = 3$ corresponds to our best estimate and places this star in a subgiant phase of evolution. A mass close to $0.8\,M_\odot$ is indicated from a track of appropriate metallicity by VandenBerg et al. (2000). However, assuming $S_H = 0$ (no collisions) results in a T_{eff}-$\log g$ combination in irreconcilable conflict with the star's known properties, both in terms of its evolutionary stage and mass.

similar to the case of the Sun. We thus refer the reader to Papers I and II for more details.

Table 3 shows how these departure coefficients translate into Fe I abundances. With a 1σ scatter of 0.05 dex in Fe II the $S_H = 0$ model is ruled out at more than 3σ. In addition to the discrepant mean values, the $S_H = 0$ model would require a significantly smaller microturbulence for Fe I ($\xi_{FeI} = 1.2\,km\,s^{-1}$), in conflict with the one derived from Fe II lines ($\xi_{FeII} = 1.7\,km\,s^{-1}$). If the stellar parameters were determined assuming $S_H = 0$ (this time using Hα as the temperature indicator which shows some dependence on gravity), the ionization equilibrium would be reached at $T_{eff} = 5550\,K$, $\log g = 4.25$ and [Fe/H] $= -2.26$ (cf. Fig. 2). Assuming a sensible stellar mass of $M = 0.8\,M_\odot$, Δ_{HIP} (as defined in the caption of Table 7) would be -54%.

4.3. The other metal-poor reference stars

On the Balmer profile temperature scale Gmb 1830, HD 19445 and HD 84937 all require an S_H close to 3. This is surprising as these stars are in different evolutionary phases and require different non-LTE corrections. In fact, the non-LTE effects in Gmb 1830 are smaller than in the Sun resulting in an abundance and gravity correction with an opposite sign from all the other stars. This turns out to reduce the star-to-star scatter significantly (cf. Fig. 4). Non-LTE effects for HD 19445 are as large as in the Sun. The differential non-LTE result thus coincides with the LTE one.

With S_H set to 3 the non-LTE corrections are generally quite small and never entail a gravity correction larger than 0.1 dex. It might come as a surprise that we are nonetheless able to remove the large discrepancies between Mg Ib and Fe I/Fe II as gravity indicators uncovered by Fuhrmann (1998a). He points out that using Fe I/Fe II results in gravities up to

Table 4. Atomic data of Fe I lines used in the analysis of the reference stars. Column 1 gives the multiplet number, Col. 2 the wavelength in Å, Col. 3 the lower excitation energy, Col. 4 the differential $\log gf$ value with respect to $\log \varepsilon(\mathrm{Fe})_\odot = 7.51$, Col. 5 the employed $\log C_6$ value. The products $\log gf\varepsilon_\odot$ that the $\log gf$ values presented here imply differ slightly from those presented in Paper II. This is because a global minimization was performed in Paper II to determine the $\log C_6$ values, whereas lines were fitted individually here on the basis of the minimization procedure. A radial-tangential approximation to macroturbulence (Gray 1977) was used for the analysis of the Sun, a Gaussian otherwise. The equivalent widths (in mÅ) in Cols. 6–10 are of low quality, but only enter the analysis in the derivation of the microturbulence. We discourage from using these values for abundance analyses.

Mult.	λ	E_{low}	$\log gf_{\mathrm{diff}}$	$\log C_6$	Procyon	Gmb 1830	HD 19445	HD 84937	HD 140283
1	5166.2	0.000	−4.18	−32.22	73		16	5	11
1	5225.5	0.110	−4.74	−32.20	33	62			
1	5247.0	0.087	−4.91	−32.21	27	57			
1	5250.2	0.121	−4.88	−32.20	26	57			
2	4347.2	0.000	−5.47	−32.16		27			
2	4427.3	0.052	−2.94	−32.15			60	36	56
2	4445.4	0.087	−5.43	−32.15	11	27			
3	4232.7	0.110	−4.96	−32.12		47			
13	6498.9	0.958	−4.64	−32.08		27			
15	5269.5	0.859	−1.34	−32.04			111	84	97
15	5328.0	0.915	−1.49	−32.03			100	74	89
15	5371.4	0.958	−1.70	−32.02			89	64	80
15	5397.1	0.915	−2.03	−32.03			73	49	64
15	5405.7	0.990	−1.84	−32.02			76	51	69
34	6581.2	1.485	−4.73	−31.96		7			
34	6739.5	1.557	−4.92	−31.91		4			
36	5194.9	1.557	−2.15	−31.83	109		34	17	
36	5216.2	1.608	−2.22	−31.82	101		27	13	22
41	4404.7	1.557	−0.18	−31.71				98	
42	4147.6	1.485	−2.15	−31.67	100			17	26
42	4271.7	1.485	−0.25	−31.70				103	
62	6151.6	2.176	−3.31	−31.72	20	22			
62	6297.8	2.223	−2.70	−31.72	46	49			
64	6082.7	2.223	−3.60	−31.70		13			
64	6240.6	2.223	−3.30	−31.71	21	21			
66	5079.2	2.198	−2.01	−31.58	92	93			
66	5198.7	2.223	−2.14	−31.59	77				
66	5250.6	2.198	−2.00	−31.61	90	87			
68	4494.5	2.198	−1.17	−31.45					36
69	4442.8	2.176	−2.79	−31.44		37			
71	4282.4	2.176	−1.06	−31.39			57	41	45
111	6421.3	2.279	−1.98	−31.71	87	91			
111	6663.4	2.424	−2.42	−31.67	60	54			
111	6750.1	2.424	−2.56	−31.68	45	46			
111	6978.8	2.484	−2.44	−31.67	53				
114	4924.7	2.279	−2.15	−31.52	73	69			
114	5049.8	2.279	−1.31	−31.54			33	18	25
114	5141.7	2.424	−2.22	−31.50	62				
116	4439.8	2.279	−3.04	−31.39	24	24			
152	4187.0	2.449	−0.66	−30.79			62	43	54
152	4222.2	2.449	−0.98	−30.80			42	26	34
152	4233.6	2.482	−0.70	−30.79			59	40	44
152	4250.1	2.469	−0.49	−30.81			72	48	53
152	4260.4	2.399	−0.01	−30.84			100	74	75
168	6393.6	2.433	−1.46	−31.65	101		22	13	15
168	6494.9	2.404	−1.25	−31.67			38	20	28
168	6593.8	2.433	−2.32	−31.66	54	57			
169	6136.6	2.453	−1.39	−31.62			26	15	18
169	6191.5	2.433	−1.46	−31.63			25	13	18
169	6252.5	2.404	−1.62	−31.64	95		18	11	12
170	5916.2	2.453	−2.90	−31.59	25				

Table 4. continued.

Mult.	λ	E_{low}	$\log gf_{\text{diff}}$	$\log C_6$	Procyon	Gmb 1830	HD 19445	HD 84937	HD 140283
206	6609.1	2.559	−2.62	−31.62	34	33			
207	6065.4	2.608	−1.46	−31.55	97	99	16	7	11
207	6137.6	2.588	−1.31	−31.57					15
207	6200.3	2.608	−2.35	−31.57	44	41			
207	6230.7	2.559	−1.16	−31.59			30	15	21
207	6322.6	2.588	−2.35	−31.58	48	44			
209	5778.4	2.588	−3.51	−31.53	7				
268	6546.2	2.758	−1.59	−31.54	81	88			8
268	6592.9	2.727	−1.47	−31.55		92			9
268	6677.9	2.692	−1.33	−31.57	100		20	11	12
318	4890.7	2.875	−0.44	−30.80			50	33	38
318	4891.4	2.851	−0.17	−30.81			67	48	54
318	4918.9	2.865	−0.38	−30.81			57	36	41
318	4920.5	2.832	0.06	−30.83			81	58	64
318	4957.2	2.851	−0.42	−30.84			56	34	39
318	4957.5	2.808	0.19	−30.85			95	67	75
342	6229.2	2.845	−2.94	−31.47	19	10			
342	6270.2	2.858	−2.57	−31.47	28	20			
383	5068.7	2.940	−1.11	−30.82			18	11	14
383	5139.4	2.940	−0.59	−30.83			44	27	21
383	5191.4	3.038	−0.61	−30.80			36	19	25
383	5232.9	2.940	−0.13	−30.86			67	45	50
383	5266.5	2.998	−0.43	−30.83			47	29	34
383	5281.7	3.038	−0.91	−30.82			22	13	14
384	4787.8	2.998	−2.62	−30.70	18				
553	5217.3	3.211	−1.03	−30.71	88	95	10	6	7
553	5253.4	3.283	−1.57	−31.31	56	44			
553	5324.1	3.211	−0.05	−30.75			50	32	36
553	5339.9	3.266	−0.62	−30.71			21	13	13
553	5393.1	3.241	−0.65	−30.75			20	11	13
554	4736.7	3.211	−0.80	−30.48	110		23	13	14
686	5586.7	3.368	−0.07	−30.71			42	27	28
686	5569.6	3.417	−0.54	−30.66			21	12	13
686	5572.8	3.396	−0.28	−30.68			32	19	21
686	5615.6	3.332	0.05	−30.74			52	33	37
686	5624.5	3.417	−0.75	−30.68	100		20	8	9
816	6232.6	3.654	−1.21	−30.67	61	44			
816	6246.3	3.602	−0.71	−30.71	89	93			6
816	6400.0	3.602	−0.25	−30.74			25	15	17
816	6411.6	3.654	−0.62	−30.71	98		13	8	9
984	4985.2	3.928	−0.71	−30.08	86	74			
1031	5491.8	4.186	−2.22	−30.53	6				
1062	5525.5	4.230	−1.28	−30.05	36				
1087	5662.5	4.178	−0.60	−30.07	75	56			
1087	5705.4	4.301	−1.49	−30.05	21	9			
1092	5133.6	4.178	0.20	−30.40			25	15	16
1094	5074.7	4.220	−0.10	−30.32	104	89	14	9	
1146	5364.8	4.445	0.15	−30.21	108	94	16	11	9
1146	5367.4	4.415	0.22	−30.25			21	14	11
1146	5369.9	4.371	0.34	−30.31			25	17	15
1146	5383.3	4.312	0.42	−30.38			30	21	20
1146	5424.0	4.320	0.52	−30.39			34	22	22
1164	5410.9	4.473	0.14	−30.20		102	19	11	13
1164	5415.1	4.386	0.41	−30.31			29	18	17
1178	6024.0	4.548	0.03	−30.40	93	71	10	6	5
1179	5855.1	4.607	−1.56	−30.26	12				
1195	6752.7	4.638	−1.27	−30.05	20				

Table 5. Atomic data of Fe II lines used in the analysis of the reference stars. Column 1 gives the multiplet number, Col. 2 the wavelength in Å, Col. 3 the lower excitation energy, Col. 4 the differential gf value with respect to $\log \varepsilon(\text{Fe})_\odot = 7.51$, Col. 5 the employed $\log C_6$ value. A radial-tangential approximation to macroturbulence (Gray 1977) was used for the analysis of the Sun, a Gaussian otherwise. The equivalent widths (in mÅ) in Cols. 6–10 are of low quality, but only enter the analysis in the derivation of the microturbulence. We discourage from using these values for abundance analyses.

mult.	λ	E_{low}	$\log gf_{\text{diff}}$	$\log C_6$	Procyon	Gmb 1830	HD 19445	HD 84937	HD 140283
27	4416.8	2.77	−2.64	−31.78		28	14	14	11
27	4233.1	2.57	−2.04	−31.78		77	44	47	47
35	5136.8	2.83	−4.44	−31.78	20				
35	5132.6	2.79	−4.17	−31.78	35				
35	5100.6	2.79	−4.18	−31.78	37				
36	4993.3	2.79	−3.73	−32.18	49				
37	4629.3	2.79	−2.38	−32.18			20	19	17
37	4582.8	2.83	−3.20	−32.18	86				
37	4555.8	2.82	−2.48	−32.18		33	18	19	17
37	4515.3	2.83	−2.53	−31.88		32	14	15	14
37	4491.4	2.84	−2.75	−31.78	108	21	9	9	
38	4620.5	2.82	−3.33	−31.78	78	8			
38	4576.3	2.83	−2.95	−31.78	96		6	6	
38	4508.2	2.84	−2.39	−31.78			18	20	16
40	6516.0	2.88	−3.29	−32.11	79				
40	6432.6	2.88	−3.61	−32.11	67				
40	6369.4	2.88	−4.19	−32.11	33				
41	5284.1	2.88	−3.11	−32.11	88	11			
42	5169.0	2.88	−1.28	−32.01			83	80	70
42	5018.4	2.88	−1.29	−32.11		96	70	72	70
42	4923.9	2.88	−1.53	−31.91		87	61	65	58
43	4656.9	2.88	−3.62	−32.11	58				
46	6084.1	3.19	−3.84	−32.19	36				
46	5991.3	3.14	−3.56	−32.19	51				
48	5362.8	3.19	−2.57	−32.19			8	8	7
48	5264.8	3.22	−3.08	−32.19	73	6			
49	5425.2	3.19	−3.27	−32.19	65				
49	5325.5	3.21	−3.21	−32.19	68				
49	5316.6	3.14	−1.91	−31.89		44	27	29	26
49	5234.6	3.21	−2.21	−31.89		28	15	16	14
49	5197.5	3.22	−2.27	−31.89		23	13	13	11
74	6456.3	3.89	−2.09	−32.18	100	11	6	7	
74	6416.9	3.87	−2.67	−32.18	63				
74	6247.5	3.87	−2.33	−32.18	89	6			
74	6239.9	3.87	−3.49	−32.18	29				
74	6149.2	3.87	−2.76	−32.18	64				

0.5 dex smaller than those from Mg Ib which are in excellent agreement with HIPPARCOS. The solution to this apparent contradiction lies in the choice of C_6 values: the larger C_6 values as proposed by Anstee & O'Mara (1991, 1995) enter our analysis via the evaluation of the strong solar Fe I lines where a certain exchange between f values and damping constants is possible (for more details on our exact choice of damping parameters see Paper II). Thus our set of *differential f* values differs systematically from that employed in the studies by Fuhrmann (1998a) and Fuhrmann (1998b, 2003) which employ C_6 values calculated using the Unsöld (1968) approximation.

We have no physical explanation for our empirical finding that hydrogen collisions are as efficient as $S_H = 3$. Laboratory measurements for the Na I resonance line at H beam energies above 10 eV indicate efficiencies as low as $S_H \approx 0.01$ (Fleck et al. 1991). We are convinced that $S_H = 3$ is not an artefact of our modelling, as the same code results in much lower efficiencies for simpler atoms like Mg or Al (Baumüller & Gehren 1996; Zhao et al. 1998). But whereas Mg I and Al I are essentially shaped by a few strong photoionization cross-sections, nearly all Fe I terms are depopulated by photoionization. This gives Fe I a unique atomic structure. In spite of the laboratory results mentioned above, it can thus not be ruled out that hydrogen collisions among Fe I terms are in fact as efficient as

Table 6. Different sets of stellar parameters for Procyon. The radius is determined from $T_{\rm eff}$ and $M_{\rm bol}$ and has to be compared with the fundamental value of $R = (2.07 \pm 0.02) R_\odot$. $\Delta_{\rm HIP} = 100 \, (d_{\rm spec} - d_{\rm HIP})/d_{\rm HIP}$.

model	$T_{\rm eff}$ [K]	log g	[Fe II/H]$_{\rm diff}$	Mass [$M_\odot$]	Radius [$R_\odot$]	$\Delta_{\rm HIP}$ [%]
1	6512	3.96	−0.09	1.42	2.13	−3.1
2	6508	3.96	−0.03	1.42	2.13	−3.0
3	6508	3.81	−0.10	1.42	2.13	+15.0
4	6600	3.96	−0.03	1.42	2.06	−0.1

1 $T_{\rm eff}$, log g, [Fe/H]: Allende Prieto et al. (2002).
2 $T_{\rm eff}$: Balmer profiles/log g: astrometry/[Fe/H]: from Fe II.
3 $T_{\rm eff}$: Balmer profiles/log g: Fe I/Fe II ($S_{\rm H} = 3$).
4 $T_{\rm eff}$: free parameter, log g: astrometry *and* Fe I/Fe II ($S_{\rm H} = 3$).

the Drawin (1968, 1969) formula predicts (or three times as efficient). We note that $S_{\rm H}$ would even be higher, if we hadn't enforced upper-level thermalization above 7.3 eV to account for term incompleteness (for details see Paper I).

Holweger (1996) uses the red giant Pollux ($\equiv \gamma$ Gem) to calibrate $S_{\rm H}$ to a value of 0.1. This result is not in direct conflict with ours as Holweger did not have access to the Bautista (1997) cross-sections for photoionization.

From the point of view of hydrodynamical model atmospheres it could be argued that the model temperatures in the outer layers of static atmospheres are overestimated (Asplund et al. 1999). Lower temperatures would predominantly make low-excitation lines of neutral species come out stronger, thus alleviating the need for strongly thermalizing collisions (high values of $S_{\rm H}$) to counterbalance photoionization. Using 2D radiation-hydrodynamical simulations, Steffen & Holweger 2002 derive granulation corrections for lines arising from low-lying levels of neutral species reaching up to −0.3 dex in the solar case. More work on combining hydrodynamical with non-LTE computations is clearly needed (cf. Shchukina & Trujillo Bueno 2001 for first attempts with respect to Fe).

4.4. Procyon

Apart from the Sun, α CMi is one of the very few stars for which the whole set of fundamental stellar parameters except metallicity is known from direct measurements. Allende Prieto et al. (2002) review recent determinations of these quantities. Its proximity ($d = (3.5 \pm 0.01)$ pc) and the presence of a white dwarf companion (Procyon B) allow to constrain Procyon's mass ($M = (1.42 \pm 0.06) M_\odot$). From the radius ($R = (2.07 \pm 0.02) R_\odot$) and measurements of the integrated flux the effective temperature is known to within ~100 K and probably lies between 6500 K and 6600 K. Mass and radius can be combined to yield the logarithmic surface gravity, log $g = 3.96 \pm 0.02$. The metallicity is close to solar. Allende Prieto et al.'s final choice for their comparative 1D static and 3D hydrodynamical modelling is $T_{\rm eff} = 6512$ K, log $g = 3.96$ and solar composition. We adopt the same value for the surface gravity and derive the effective temperature from the Balmer lines which yield an average value of $T_{\rm eff} = (6508 \pm 60)$ K. The evolutionary tracks

of VandenBerg et al. (2000) point towards a somewhat higher mass of 1.52 $M_\odot$, in better agreement with the mass estimate of Girard et al. (2000) who also consider ground-based measurements for the angular separation of Procyon A and B. To be able to compare our results directly to those of Allende Prieto et al. (2002), we stick to the choice of parameters given above. We note, however, that this choice of mass produces a 3% offset with respect to HIPPARCOS.

It turns out that our model is not able to fulfil the ionization equilibrium of iron with $S_{\rm H} = 3$. With differential non-LTE effects in abundance of merely 0.01 dex the unbalance amounts to Δ (Fe II − Fe I) = 0.07 dex. To remove this discrepancy this model would require a gravity of log $g = 3.81$, many standard deviations away from the astrometric result.
How would one have to tune $S_{\rm H}$ to remove Δ (Fe II − Fe I)? Surprisingly, no choice of $S_{\rm H}$ is able to fulfil the ionization equilibrium. Using the largest non-LTE corrections possible ($S_{\rm H} = 0$) the discrepancy is merely reduced by 0.02 dex. In this sense Procyon only documents our failure to use this star as a calibrator for $S_{\rm H}$.

Seemingly, Allende Prieto et al. (2002) are more successful with their 1D LTE modelling of Procyon's iron spectrum. Their Δ (Fe II − Fe I) amounts to 0.02 dex in log ε(Fe) (log ε(Fe I) = 7.30 $\pm$ 0.11 vs. log ε(Fe II) = 7.32 $\pm$ 0.08) or 0.04 dex in log g. Upon closer inspection one notices that these values are *non-differential* abundances. Formulated relative to the Sun where a discrepancy of 0.06 dex was obtained by these authors, the discrepancy in Procyon rises to 0.08 dex which is in complete numerical agreement with our LTE result. Irrespective of whether one prefers differential analyses or not, we conclude that Allende Prieto et al. (2002) do not master iron in this star, either (their 3D hydrodynamical modelling results in a residual trend of log ε (Fe I) with line strength which could be removed by including a microturbulence of $\xi \approx 0.3$ km s^{-1}).

Steffen (1985) investigated different ionization equilibria in Procyon and drew the conclusion that the fundamental temperature needs to be revised upwards by more than 200 K. Alternatively, the gravity would have to be lowered to log $g \simeq 3.55$ which can be ruled out by astrometry. In the framework of non-LTE modelling, a similar temperature correction would be required to bring [O I 6300] into concordance with the IR triplet lines (Reetz 1999). We can follow along this track and seek the temperature at which the $S_{\rm H} = 3$ model brings log ε(Fe I) into concordance with log ε(Fe II) without contradicting the astrometric distance constraint. This temperature is found to be $T_{\rm eff} = 6600$ K or 90 K higher than our best spectroscopic estimate based on Balmer profiles. As can be appreciated from inspecting Fig. 3 this temperature is in conflict with the Balmer profile analysis. It is, however, in not in disagreement with the gravity inferred from the Mg Ib lines when employing the non-LTE model atom for magnesium presented by Zhao et al. (1998). This is because the strong-line method is not very sensitive to changes in temperature. Thus, while disquieting on the whole, our result is an improvement over the analysis of Steffen (1985). Higher temperatures for Procyon certainly seem possible in view of the Strömgren photometry of Edvardsson et al. (1993, $T_{\rm eff} = 6705$ K) and the IRFM temperature of Alonso et al. (1996, $T_{\rm eff} = 6631$ K). From

Table 7. Stellar parameters derived using Fe I/II in non-LTE as a gravity indicator with $S_H = 3$. The spectroscopic distance d_{spec} is calculated from $\log \pi_{spec} = 0.5\,([g] - [M]) - 2\,[T_{eff}] - 0.2\,(V + BC + A_V + 0.25)$, where $[X] = \log(X/X_\odot)$. $\Delta_{HIP} = 100\,(d_{spec} - d_{HIP})/d_{HIP}$. The oxygen abundance is derived by means of profile analysis of the IR triplet in non-LTE (Reetz 1999), the magnesium abundance from profiles of weak optical lines in non-LTE ($\lambda\lambda$ 4571, 4702, 4730, 5528, 5711 Å, Zhao et al. 1998).

Object	T_{eff} [K]	$\log g$	[Fe/H] NLTE	[O/Fe] NLTE	[Mg/Fe] NLTE	Mass [$M_\odot$]	A_V [mag]	BC [mag]	d_{spec} [pc]	d_{HIP} [pc]	Δ_{HIP} [%]
HD 103095	5070	4.66	−1.36	+0.63	+0.21	0.62	0.00	−0.32	8.86	9.16	−3.2
HD19445	6032	4.40	−2.08	+0.68	+0.49	0.67	0.00	−0.21	38.80	38.68	0.3
HD 140283	5806	3.68	−2.43	+0.71	+0.26	0.79	0.13	−0.23	56.60	57.34	−1.3
HD 84937	6346	4.00	−2.16	+0.59	+0.39	0.79	0.11	−0.18	80.34	80.39	−0.1
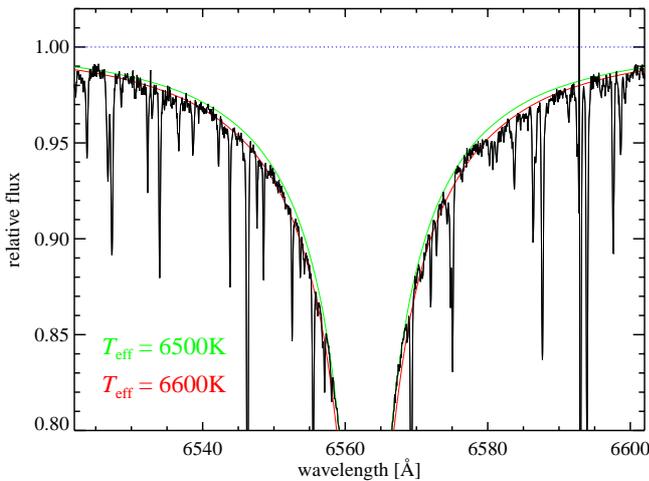
Fig. 3. Profile fits to Hα in the FOCES spectrum of Procyon. The revised temperature ($T_{eff} = 6600$ K) is in disagreement with the observations.

the new self-broadening theory for Balmer lines presented by Barklem et al. (2000) higher temperatures ($T_{eff} = 6570$ K) are possible, *if* the zero-point offset for the Sun is properly accounted for.

5. Stellar parameters from the $S_H = 3$ model

Having calibrated S_H, we reanalyse the iron spectra of the reference stars with our non-LTE model for iron. The final parameters are given in Table 7.

Figure 4 compares the stellar parameters in non-LTE with their LTE counterparts. In particular, the scatter is reduced in going from LTE to non-LTE, as differential non-LTE effects for HD 103095 bear the opposite sign to those of all the other stars. Non-LTE corrections are largest for HD 84397 and HD 140283. A positive slope of a linear regression line in this diagram would thus indicate underestimated non-LTE correction and vice versa. This effect will be seen in the analyses of Thévenin & Idiart (1999) and Fulbright (2000) below.

5.1. Comparison with other studies

Based on our newly established methodology, we can now compare the resulting spectroscopic distance scale with that of other studies. We compare the residual offset with respect
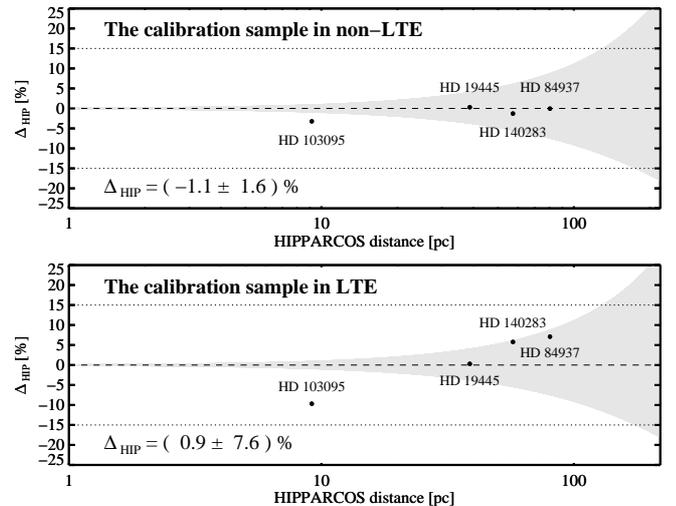

Fig. 4. Δ_{HIP} as a function of the astrometric distance, both in non-LTE (top) and LTE (bottom). The grey wedge indicates the typical uncertainty of the HIPPARCOS parallaxes. When non-LTE gravities are considered the star-to-star scatter is significantly reduced.

to the HIPPARCOS astrometry and the star-to-star scatter for the – admittedly – small sample of reference stars. For a fair and valid comparison, we use the published stellar parameters, but rederive bolometric corrections and masses. Since an estimate for the [α/Fe] ratio is needed for interpolating among appropriate evolutionary tracks, we only consider studies which supply an α-element abundance alongside [Fe/H]. We therefore disregard e.g. the study of Soubiran et al. (1998).

Particular attention is paid to studies which also undertook kinetic equilibrium calculations for iron. As can be appreciated from comparing the upper panel of Figs. 4 to 5, all studies using Fe I/Fe II are an order of magnitude less precise than our calibration.

5.1.1. Gratton et al. (1999)

These authors employ a rather simplistic model atom of Takeda (1991), treat the Fe I photoionization and background opacities empirically and calibrate S_H by means of RR Lyrae stars. As S_H is determined to be 30, thermal populations result for their stars which is why the LTE stellar parameters of Gratton et al. (1996) are still the basis for the analysis of Carretta et al. (2000). Due to the dominant influence of oxygen on the
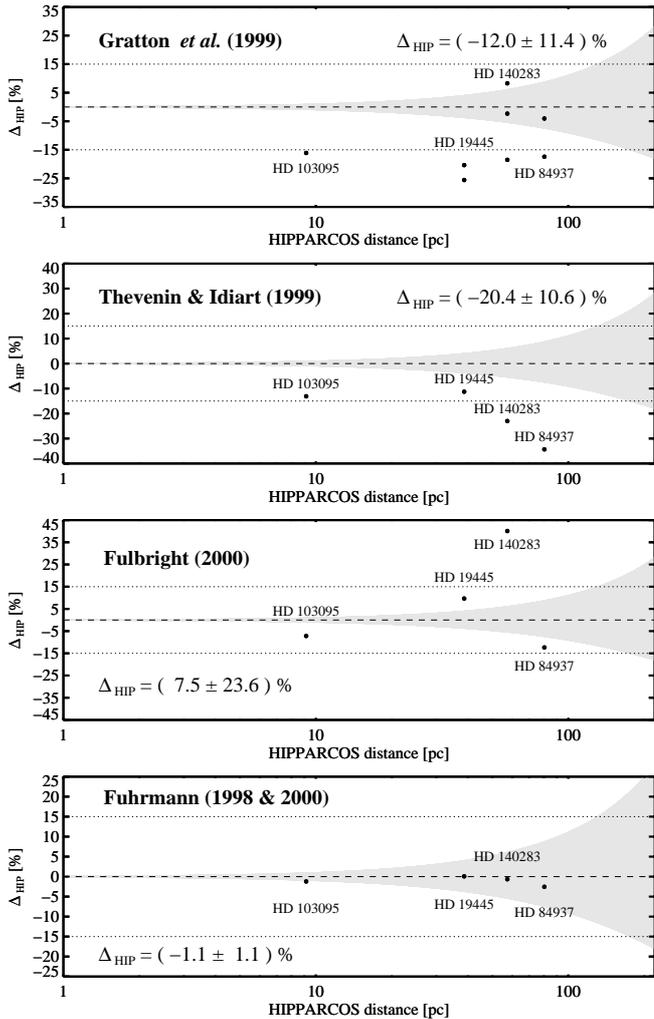
Fig. 5. Same as Fig. 4, here for the studies discussed in the text. Note the different y-axis scales. Except for the work of Fuhrmann (1998b, 2000), all studies show large star-to-star scatter and/or offsets with respect to HIPPARCOS.

morphology of the evolutionary tracks, we use their published $[O/Fe]_{NLTE}$ as $[\alpha/Fe]$.

The topmost panel of Fig. 5 shows the resulting spectroscopic distance scale in comparison with the astrometric distances of HIPPARCOS. Since the temperatures these authors derive via the IRFM are in excellent agreement with ours, it is surprising to see that the gravities are somewhat overestimated rather than underestimated. From the work of Fuhrmann et al. (1997) we would have expected the LTE gravities to be significantly too low (cf. Introduction). Since we have shown this effect to be mainly due to an inappropriate choice of damping parameters C_6, we assume that a similar effect is at work in the analyses of Gratton et al. (1996). More worrying than the 12% offset is the large scatter, e.g. in the multiple analysis of HD 140283 which amounts to nearly 30%.

5.1.2. Thévenin & Idiart (1999)

In an attempt to model the kinetic equilibrium of iron ab initio, Thévenin & Idiart (1999) put together a comprehensive and

up-to-date model atom which is quite comparable to the one used by us. Photoionization is treated according to the calculations of Bautista (1997), UV line opacities are crudely represented by a scaling rule for continuous opacities. In combination with their neglect of hydrogen collisions ($S_H \equiv 0$), these assumptions lead to very large non-LTE corrections. For example, the gravity correction for HD 140283 is calculated to be 0.54 dex. We use the larger value of $[Mg/Fe]_{NLTE}$ and $[Ca/Fe]_{NLTE}$ from Idiart & Thévenin (2000) as an estimate of $[\alpha/Fe]$.

On the temperature scale employed by these authors, the non-LTE corrections are clearly overestimated, severely so in the case of HD 84937 ($\Delta_{HIP} = -34\%$). While the scatter is comparable to that of Gratton et al. (1999), the offset is significantly larger: the sample distances are incompatible with HIPPARCOS at the 2σ level.

These authors also analyse Procyon. At a temperature of $T_{eff} = 6631$ K the ionization equilibrium of iron is reached at a gravity of $\log g = 4.00$ without departures from LTE. Judging from our own calculations (cf. Sect. 4.4) this modelling success is not surprising and basically the result of choosing a high effective temperature. The derived parameters yield $\Delta_{HIP} = -3.3\%$. Including this star into the sample, the mean offset would be reduced to 17% with the scatter increasing to 12%.

5.1.3. Fulbright (2000)

This analysis of 168 mostly metal–poor stars rests almost entirely on iron as a plasmadiagnostic tool: the temperature determination is based on the LTE excitation equilibrium of Fe I, gravity and metallicity are inferred from the LTE ionization equilibrium of Fe I/Fe II. These steps are iterated until $\log \varepsilon(Fe\ I)$ matches $\log \varepsilon(Fe\ II)$ to "within 0.03 dex in most cases". At best, we can therefore expect an accuracy for $\log g$ of 0.05 dex. We use $[Mg/Fe]_{LTE}$ as a proxy for $[\alpha/Fe]$. The masses we derive from Fulbright's stellar parameters show a wide range: HD 103095 would be a very low-mass object ($M = 0.45\,M_\odot$), HD 140283 a star of nearly solar mass ($M = 0.95\,M_\odot$). This might indicate unrealistic combinations of T_{eff} and $\log g$.

While the sample mean comes out relatively close to HIPPARCOS, the star-to-star scatter is very large. The offset for HD 140283 is 40%. Statistically speaking, the gravities are only know to within 0.25 dex. Just like in the case of Thévenin & Idiart (1999) not a single star falls in the 1σ uncertainty range of the HIPPARCOS astrometry. All this means that Fulbright's methods fail to give consistent results for metal-poor F and G stars.

5.1.4. Fuhrmann (1998b, 2000)

These studies are methodologically closest to our own, in the sense that Fuhrmann employs the same model atmosphere and the same Balmer profile temperature scale. The pressure-broadened wings of Mg Ib in LTE are used as a gravity indicator with the remarkable result of $\Delta_{HIP} = (2 \pm 5)\%$ for 100 stars. Balmer profiles and Mg Ib lines are practically orthogonal

methods to determine T_{eff} and $\log g$ which helps to prevent disadvantageous propagation of errors. Masses are interpolated among tracks of Bernkopf (1998). The stellar parameters of HD 140283 are revised with respect to Fuhrmann (1998a) and are private communication.

When using the tracks of VandenBerg et al. (2000) the resulting distances are slightly shorter than with the Bernkopf (1998) tracks. The internal consistency is, however, still very impressive. Fuhrmann's work clearly demonstrates the capabilities of a careful, differential analysis in LTE.

We note in passing that the revision of the stellar mass for Procyon (down to $M = 1.42\,M_{\odot}$) worsens the spectroscopic result published by Fuhrmann (1998b) to $\Delta_{HIP} = -9.6\%$. Thus Procyon still is a paramount test case for any spectroscopic analysis.

6. Extreme applications: HE 0107–5240 and CS 29497–004

In the meantime, our model has been applied to a couple of new extreme halo objects: HE 0107−5240, the most iron-deficient star currently known (Christlieb et al. 2002) and CS 29497−004, a new highly *r*-process enhanced star (Christlieb et al. 2003). Since both objects are on the upper red giant branch (RGB), non-LTE corrections to gravity are larger than in the case of the reference stars discussed above.

Both stars have effective temperatures around 5100 K and surface gravities around 2.2. Despite their vastly different metallicities ([Fe/H] = −5.3 vs. −2.6), non-LTE corrections to gravity are very similar and amount to +0.3 dex. They are similar because two competing processes cancel each other. On the one hand, the Fe I departure coefficients of HE 0107−5240 are more extreme than those of CS 29497−004; on the other, the Fe I lines in HE 0107−5240 are much weaker and therefore originate deeper in the atmosphere. As test calculations have shown, hydrogen collisions are still important to consider at these RGB gravities.

Further calculations indicate that non-LTE effects in Fe I reach a plateau value below a metallicity comparable to that of the most metal-poor globular clusters found in our Galaxy. Globular cluster giants are thus ideal targets to verify the predictions of our calculations. It is encouraging to see that at intermediate metallicities these predictions are in good agreement with the mild Fe I/Fe II imbalance found in the LTE analyses of giants in M 5 and M 71 by Ramírez & Cohen (2003).

7. Conclusions

We have presented a procedure to determine the poorly-known efficiency of collisions with neutral hydrogen in our kinetic equilibrium calculations for the formation of Fe I and Fe II lines in the atmospheres of solar-type stars. This procedure rests on exploiting the astrometric constraint of HIPPARCOS parallaxes. The scaling factor S_H is determined to be 3 which makes hydrogen collisions the most important atomic process counterbalancing the otherwise overwhelming photoionization in metal-poor stars. We emphasize, however, that our goal has not been to determine the absolute strength of hydrogen collisions.

Rather, our analysis is aimed at removing biases that are present in the analysis of metal-poor stars when using the iron ionization equilibrium in LTE using 1D model atmospheres.

For a representative sample of local halo stars the combination of Balmer profile temperatures and non-LTE iron ionization equilibrium gravities succeeds in fulfilling the astrometric constraint. Other authors (Gratton et al. 1999; Thévenin & Idiart 1999; Fulbright 2000) present results an order of magnitude less accurate. This underlines our claim that hydrogen collisions must be considered in kinetic equilibrium calculations. The independent method to derive $\log g$ used by Fuhrmann (1998b, 2000) yields comparable results.

Our method cannot establish the ionization equilibrium of Procyon at the fundamental parameters $T_{eff} = 6510$ K and $\log g = 3.96$. An upward revision of Procyon's temperature by 90 K (1.3%) to $T_{eff} = 6600$ K is indicated instead, in agreement with the radius determination based on its bolometric magnitude. This temperature is, however, in disagreement with the spectroscopic constraint of the Balmer profiles.

Using our carefully calibrated model of Fe I/Fe II, cool stars over the whole range of metallicities encountered in the Galaxy can now be analysed in a homogeneous way with reduced methodological biases without resorting to trigonometric parallaxes.

References

Ali, A. W., & Griem, H. R. 1965, Phys. Rev., 140, 1044
Ali, A. W., & Griem, H. R. 1966, Phys. Rev., 144, 366
Allende Prieto, C., Asplund, M., García López, R. J., & Lambert, D. L. 2002, ApJ, 567, 544
Alonso, A., Arribas, S., & Martínez-Roger, C. 1996, A&AS, 117, 227
Anstee, S. D., & O'Mara, B. J. 1991, MNRAS, 253, 549
Anstee, S. D., & O'Mara, B. J. 1995, MNRAS, 276, 859
Asplund, M., Nordlund, Å., Trampedach, R., & Stein, R. F. 1999, A&A, 346, L17
Asplund, M., Nordlund, Å., Trampedach, R., & Stein, R. F. 2000, A&A, 359, 743
Baumuller, D., & Gehren, T. 1996, A&A, 307, 961
Barklem, P. S., Piskunov, N., & O'Mara, B. J. 2000, A&A, 363, 1091
Bernkopf, J. 1998, A&A, 332, 127
Bautista, M. A. 1997, A&AS, 122, 167
Böhm-Vitense, E. 1958, Z. Astrophys., 46, 108
Carlsson, M., Rutten, R. J., & Shchukina, N. G. 1992, A&A, 253, 567
Carretta, E., Gratton, R. G., & Sneden, C. 2000, A&A, 356, 238
Christlieb, N., Bessell, M. S., Beers, T. C., et al. 2002, Nature, 419, 904
Christlieb, N., et al. 2003, ApJ, submitted
Drawin, H. W. 1968, Z. Phys., 211, 404
Drawin, H. W. 1969, Z. Phys., 225, 483
Edvardsson, B., Anderson, J., Gustafsson, B., et al. 1993, A&A, 275, 101

ESA 1997, The Hipparcos and Tycho Catalogues, ESA SP-1200

Fleck, I., Grosser, J., Schenke, A., Steen, W., & Voigt, H. 1991, J. Phys. B, 24, 4017

Fuhrmann, K. 1998a, A&A, 330, 626

Fuhrmann, K. 1998b, A&A, 338, 161

Fuhrmann, K. 2000, A&A, submitted

Fuhrmann, K. 2003, AN, submitted

Fuhrmann, K., Axer, M., & Gehren, T. 1993, A&A, 271, 451

Fuhrmann, K., Pfeiffer, M., Frank, C., Reetz, J., & Gehren, T. 1997, A&A, 323, 909

Fulbright, J. P. 2000, AJ, 120, 1841

Gehren, T., Butler, K., Mashonkina, L., Reetz, J., & Shi, J. 2001a, A&A, 366, 981 (Paper I)

Gehren, T., Korn, A. J., & Shi, J. 2001b, A&A, 380, 645 (Paper II)

Girard, T. M., Wu, H., Lee, J. T., et al. 2000, AJ, 119, 2428

Gratton, R. G., Carretta, E., & Castelli, F. 1996, A&A, 314, 191

Gratton, R. G., Carretta, E., Eriksson, K., & Gustafsson, B. 1999, A&A, 350, 955

Gray, D. F. 1977, ApJ, 218, 530

Hauck, B., & Mermilliod, M. 1998, A&AS, 129, 431

Holweger, H. 1996, Phys. Scr. T, 65, 151

Idiart, T., & Thévenin, F. 2000, ApJ, 541, 297

Korn, A. J. 2002, in Scientific Drivers for ESO Future VLT/VLTI Instrumentation, ed. J. Bergeron, & G. Monnet, ESO Astrophysics Symposia (Heidelberg: Springer), 199

Kurucz, R. L. 1992, Rev. Mex. Astron. Astrof., 23, 45

Kurucz, R. L., Furenlid, I., Brault, J., & Testerman, L. 1984, Solar Flux Atlas from 296 to 1300 nm, Kitt Peak National Solar Observatory

Lambert, D. L. 1993, Phys. Scr. T, 47, 186

Peterson, R. C., Dorman, B., & Rood, R. T. 2001, ApJ, 559, 372

Pfeiffer, M. J., Frank, C., Baumüller, D., Fuhrmann, K., & Gehren, T. 1998, A&AS, 130, 381

Ramírez, S. V., & Cohen, J. G. 2003, ApJ, 125, 224

Reetz, J. K. 1999, Ph.D. Thesis, Ludwig-Maximilians-Universität München

Shchukina, N., & Trujillo Bueno, J. 2001, ApJ, 550, 970

Soubiran, C., Katz, D., & Cayrel, R. 1998, A&AS, 133, 221

Steenbock, W., & Holweger, H. 1984, A&A, 130, 319

Steffen, M. 1985, A&AS, 59, 403

Steffen, M., & Holweger, H. 2002, A&A, 387, 258

Takeda, Y. 1991, A&A, 242, 455

Thévenin, F., & Idiart, T. P. 1999, ApJ, 521, 753

Unsöld, A. 1968, Physik der Sternatmosphären (Berlin-Heidelberg-New York: Springer-Verlag)

VandenBerg, D. A., Swenson, F. J., Rogers, F. J., Iglesias, C. A., & Alexander, D. R. 2000, ApJ, 532, 430

van Regemorter, H. 1962, ApJ, 136, 906

Vidal, C. R., Cooper, J., & Smith, E. W. 1970, JQSRT, 10, 1011

Zhao, G., Butler, K., & Gehren, T. 1998, A&A, 333, 219